

# Development of Bulk Optical Negative Index Fishnet Metamaterials: Achieving a Low-Loss and Broadband Response Through Coupling

*This paper deals with design, fabrication, and characterization of “fishnet” structures for building broadband low-loss negative-refraction metamaterials and shows how coupling of unit cells improves the results.*

By JASON VALENTINE, SHUANG ZHANG, THOMAS ZENTGRAF, AND XIANG ZHANG

**ABSTRACT** | In this paper, we discuss the development of a bulk negative refractive index metamaterial made of cascaded “fishnet” structures, with a negative index existing over a broad spectral range. We describe in detail the design of bulk metamaterials, their fabrication and characterization, as well as the mechanism of how coupling of the unit cells can reduce loss in the material through an optical transmission-line approach. Due to the lowered loss, the metamaterial is able to achieve the highest figure of merit to date for an optical negative index metamaterial (NIM) in the absence of gain media. The increased thickness of the metamaterial also allows a direct observation of negative refraction by illuminating a prism

made of the material. Such an observation results in an unambiguous demonstration of negative phase evolution of the wave propagating inside the metamaterial. Furthermore, the metamaterial can be readily accessed from free space, making it functional for optical devices. As such, bulk optical metamaterials should open up new prospects for studies of the unique optical effects associated with negative and zero index materials such as the superlens, reversed Doppler effect, backward Cerenkov radiation, optical tunneling devices, compact resonators, and highly directional sources.

**KEYWORDS** | Metamaterials; nanoscale materials; negative index; optics

Manuscript received July 21, 2010; revised September 23, 2010; accepted October 31, 2010. Date of publication January 28, 2011; date of current version September 21, 2011. This work was supported by the U.S. Army Research Office (ARO) MURI program 50432-PH-MUR and in part by the National Science Foundation (NSF) Nano-Scale Science and Engineering Center CMMI-0751621.

**J. Valentine** was with the National Science Foundation (NSF) Nano-Scale Science and Engineering Center (NSEC), University of California Berkeley, Berkeley, CA 94720 USA. He is now with the Mechanical Engineering Department, Vanderbilt University, Nashville, TN 37240 USA (e-mail: jason.g.valentine@vanderbilt.edu).

**S. Zhang** was with the National Science Foundation (NSF) Nano-Scale Science and Engineering Center (NSEC), University of California Berkeley, Berkeley, CA 94720 USA. He is now with the School of Physics and Astronomy, University of Birmingham, Edgbaston, Birmingham B15 2TT, U.K. (e-mail: s.zhang@bham.ac.uk).

**T. Zentgraf** is with the National Science Foundation (NSF) Nano-Scale Science and Engineering Center (NSEC), University of California Berkeley, Berkeley, CA 94720 USA (e-mail: zentgraf@me.berkeley.edu).

**X. Zhang** is with the National Science Foundation (NSF) Nano-Scale Science and Engineering Center (NSEC), University of California Berkeley, Berkeley, CA 94720 USA and also with the Material Sciences Division, Lawrence Berkeley National Laboratory, Berkeley, CA 94720 USA (e-mail: xzhang@me.berkeley.edu).

Digital Object Identifier: 10.1109/JPROC.2010.2094593

## I. INTRODUCTION

Since the inception of negative index metamaterials (NIMs) in the microwave region [1], [2] there has been a constant drive to lower the operating wavelength into the optical regime [3]–[5]. A negative refractive index is not exhibited in naturally occurring materials due to lack of a high-frequency magnetic response. The ability to tune both the permeability and permittivity of a material allows scientists, for the first time, to fully explore the parameter space of electromagnetic properties. Achieving a material with a negative refractive index at optical frequencies is perhaps the most challenging implementation of the metamaterial concept as it requires engineering both

negative permeability and permittivity in the same spectral region. However, such a material could lead to a number of new optical devices such as super-resolution lenses [6] and highly directional sources [7]. The optical regime is also particularly interesting due to the presence of several attractive areas of application of such devices including telecommunications, biological imaging/sensing, and lithography. However, there have been both fundamental and engineering challenges in scaling such metamaterials to optical wavelengths. On a fundamental level, the increased loss and penetration depth in metals at optical frequencies causes metamaterials to absorb a large proportion of the incident light. This absorption is further increased by the resonant nature of most NIMs. Another fundamental challenge arises from the fact that at short wavelengths, we start to approach the plasma frequency of metals, causing saturation in the magnetic response of the structure [8], [9]. As such, the figure of merit (FOM) for optical negative index metamaterials is defined as  $-\text{Re}(n)/\text{Im}(n)$  and describes the number of oscillations that light undergoes inside the material before being absorbed [10].

Despite the previous demonstrations of optical negative index metamaterials [3]–[5], a monolayer of unit cells along the propagation direction does not allow the investigation of the interesting physics associated with negative phase propagation. Thick materials are highly desirable so that the overall geometry of the material can be used to manipulate light propagation such as in a lens or prism [11]. These effects are directly connected to the shape of the surface and the propagation length for different spatial paths of the beam. For a monolayer or a thin film it is simply not possible to form a thick object such as a lens to manipulate the flow of light. However, on the engineering level, it becomes difficult to fabricate thick metamaterials with the

proper dimensionality at optical frequencies. For instance, at such short wavelengths, nanoscale imperfections are at the scale of the incident radiation, causing scattering loss and reduced material performance. This challenging scale level also makes it difficult to fabricate thick metamaterials while maintaining the requisite nanoscale unit cell geometries.

Among the most popular designs of optical NIMs is the so-called “fishnet” structure. The fishnet can be thought of as a combination of two separate constituents, which allow the permeability and permittivity of the structure to be engineered independently [12]. The first component of the fishnet metamaterial is thick metallic strips oriented along the direction of magnetic field of the incoming light which are separated by a dielectric layer [Fig. 1(a)]. This structure functions as an inductor and capacitor resonator wherein antisymmetric currents are created in the metal strips, which give rise to an induced magnetic polarization in the structure [Fig. 1(e)]. This provides a magnetic response, or artificial permeability, that can achieve negative values near resonance. The second constituent consists of thin metallic wires oriented in the direction of the electric field of the incoming light [Fig. 1(b)]. These wires function as a diluted metal with decreased plasma frequency, providing a negative effective permittivity that can be engineered separately from the permeability. These two constituents are combined to form the fishnet metamaterial where both the negative permeability and permittivity can be engineered at a particular wavelength [Fig. 1(c) and (d)]. An alternative explanation of the negative refraction arising from multilayer fishnet metamaterials is based on the spoof plasmon [13] supported by each perforated metallic film [14], [15]. While it describes the identical response as the constituent model, the spoof plasmon model can provide additional insight into the underlying physics. It is found that the coupling of the spoof

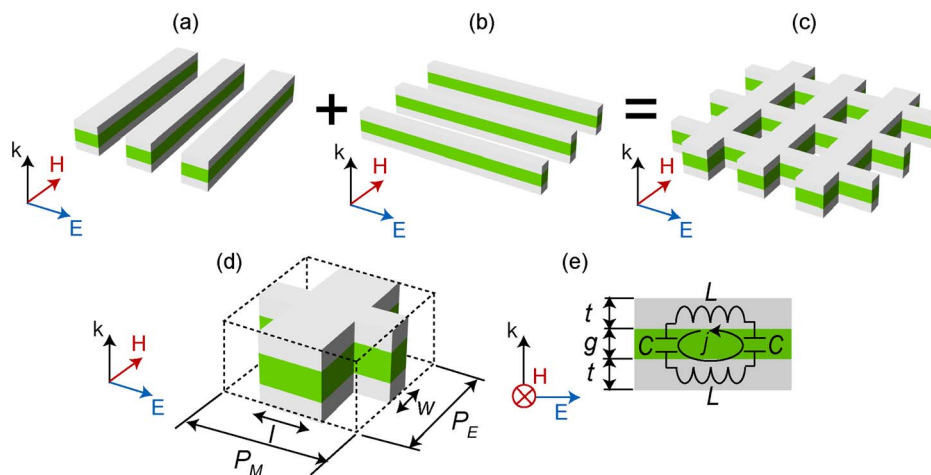


**Fig. 1.** Fishnet metamaterial schematic showing a single functional layer (metal/dielectric/metal) (a) and (b) schematics of the separate constituents of the metamaterial which provide both (a) magnetic and (b) electric response. The gray layers are made of metal and the green layer a dielectric. Combined (c), these constituents form the complete fishnet structure. (d) Unit cell geometry of the metamaterial. (e) Depicts the LC circuit and current loop that form the magnetic response in the fishnet metamaterial.

plasmon leads to a negative dispersion over a certain frequency range. In this sense, multilayer fishnet metamaterials effectively function as a 3-D plasmon crystal, wherein the apertures play an important role in determining the spoof plasmon dispersion, coupling the incident light into plasmon modes, and mediating the coupling among different perforated metal layers. This alternative view shows the crucial role that the surface plasmons play in achieving negative refraction. It is also important to note that while the electric field of light is mainly concentrated in the air voids of the fishnet metamaterial, the magnetic field is concentrated within the metal / dielectric stack. The spatial separation of field concentration is due to the strong magnetic response of the structure and distinguishes it from a waveguide array wherein both the electric and magnetic fields are confined in the air apertures.

The highest figure of merit for a single functional layer of the fishnet structure (one metal/dielectric/metal layer) that has been experimentally obtained is 3.0 at a wavelength of  $1.5 \mu\text{m}$  [16]. The fishnet metamaterial has also been successful at scaling the response into the visible region, however, such structures suffer from considerable loss and a low FOM [17], [18]. The shortest wavelength that the negative index fishnet metamaterial has been demonstrated is 580 nm, where a FOM of 0.3 was achieved [17].

Here, we will discuss how bulk metamaterials, and in particular the bulk fishnet metamaterial, can increase the FOM of NIMs [19]. This is possible by introducing strong interactions between the layers in the form of magneto-inductive coupling and destructive interference of surface currents. We will also demonstrate how a prism of this thick metamaterial can be used to visualize and measure the index of refraction.

## II. BULK FISHNET METAMATERIAL

It is important to begin by defining what a bulk metamaterial entails. The definition of bulk properties has been well established in solid state physics. Here, the convergence of the material properties is required for defining “bulk” as well as the requirement that the surface atomic layers do not affect the overall property of the system. A well-known example is the intensely studied topic of graphene. Bilayer graphene has different properties from a monolayer because of the interaction between the layers. By adding more layers, the properties of the multilayer graphene gradually converge wherein after a certain number of layers it can be called “graphite.” Graphite, therefore, has different properties from the single-layer graphene. Likewise, a metamaterial must also be held to this standard to be defined as bulk. In addition, it is only strictly meaningful to assign properties of a bulk material when the effective properties are not altered by the environment. A single or a few functional layers of fishnet metamaterials cannot be considered as bulk since its properties are significantly affected by the substrate.

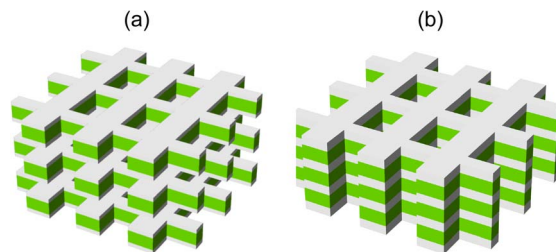


**Fig. 2. Schematic of weakly and strongly coupled metamaterials, shown here with three functional layers. (a) Weakly coupled metamaterial. (b) Strongly coupled metamaterial.**

In stacking functional layers of a metamaterial, the layers can be either weakly coupled [Fig. 2(a)] or strongly coupled [Fig. 2(b)] [20]. In the weakly coupled case, the layers are spaced far enough away that they have little interaction with one another. In this case, the properties will converge quickly and the metamaterial will essentially have the same properties as a single layer. This is more like a gas phase system, where the interactions among “molecules” are negligible. In the strongly coupled case, the functional layers are stacked at close spacing, introducing strong coupling between the layers. Such a structure may require several layers to converge to the bulk properties of the metamaterial, however, additional benefits, such as lowered loss and increased bandwidth, can be obtained. This strongly coupled case is similar to the concept of a transmission line in the microwave region [21]–[23]. Such transmission lines have successfully proven to give a nonresonant based negative refractive index with low loss for the transmission of electromagnetic waves. It is also well known that the transmission line properties cannot be the same as a single unit cell, which is a resonant structure. This strongly coupled structure with converged properties is what is referred to as a bulk metamaterial in this report.

Over the past several years, researchers have made progress in achieving bulk properties for metamaterials at optical wavelengths. In particular, fishnet metamaterials with three and five functional layers [24], [25] have been realized as well as split ring resonator metamaterials with up to four layers [26]. In all these reports, a shift in the optical properties with an increased number of stacking layers is evident; however, a converged index is not demonstrated. There have also been recent reports on anisotropic materials that exhibit negative refraction at optical frequencies due to a hyperbolic dispersion relation [27], [28]. While these materials can be made considerably thick, on the order of tens of micrometers, they do not possess a negative refractive index due to the lack of negative phase propagation.

## III. METAMATERIAL DESIGN

To acquire a clear understanding of the bulk metamaterial’s optical response, simulations were performed with a rigorous coupled wave analysis (RCWA). RCWA expands

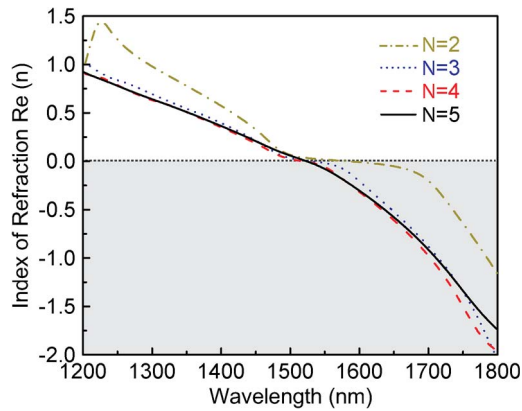


**Fig. 3. Refractive index versus number of functional layers. While a large shift is seen when increasing from two to three layers, subsequent thickness increases have no effect on the index, indicating that the bulk value has been reached.**

the electromagnetic field into a number of diffraction orders and matches the boundary conditions at each interface. The fishnet was designed to achieve a negative refractive index around  $1.5 \mu\text{m}$ . Silver (Ag) and magnesium fluoride ( $\text{MgF}_2$ ) were used as the metal and dielectric (gray and green in Fig. 1, respectively). Ag was chosen due to its relatively low intrinsic losses at optical frequencies while  $\text{MgF}_2$  was chosen due to its smooth film quality and ease of deposition. The dimensions of the structure, corresponding to Fig. 1(d), are:  $P_M = P_E = 860 \text{ nm}$ ,  $l = 565 \text{ nm}$ ,  $w = 265 \text{ nm}$ ,  $t = 30 \text{ nm}$ , and  $g = 50 \text{ nm}$ . The functional layers are stacked directly on top of one another and the refractive index was calculated for different numbers of stacked functional layers (Fig. 3). The index was found by calculating the complex transmittance and reflectance using RCWA with  $13 \times 13$  diffractive orders and solving for the Fresnel equation:  $\cos(nkd) = (1 + t^2 - r^2)/2t$ . It can be seen that after stacking three functional layers, the index is well converged to the bulk value of the metamaterial. This convergence is also observed for the

imaginary part of the refractive index and represents a collapse to the singular Bloch mode index of the material [29].

To better understand the microscopic response of the bulk fishnet structure, finite difference time domain (FDTD) simulations were performed. In all simulations, a mesh size of  $10 \text{ nm}$  was employed. First, the cascading of the layers leads to a strong magneto-inductive coupling between neighboring functional layers, as deduced from the circuit diagram in Fig. 4(b). The tight coupling between adjacent L-C resonators through mutual inductance results in a broad band negative index of refraction with low loss, which is similar to the material response of left-handed transmission lines. In addition, the loss is further reduced due to the destructive interference of the antisymmetric currents across the metal film, effectively canceling out the current flow in the center of the film. In Fig. 4(c), it can be observed that the electric field on the top and bottom surface is antisymmetric leading to the cancellation of electric field in the middle of each metal layer. As we will see, the destructive interference of the field along with the magneto-inductive coupling will lead to greatly reduced loss and increased FOM in the bulk fishnet metamaterial.

#### IV. FABRICATION

One of the largest challenges in realizing the bulk fishnet structure is fabricating a thick structure with high aspect ratio. Previous single-layer metamaterials have been typically fabricated using electron beam lithography (EBL) and a liftoff process. While this process is ideal for thin films, it is difficult to fabricate high aspect ratio structures. To make higher aspect structures, one has to perform multiple exposure/deposition/liftoff steps where each subsequent exposure must be aligned to the first. Using multiexposure EBL, researchers have made progress fabricating thicker optical NIMs with up to five functional layers having been demonstrated [25]. However, thicker materials become increasingly more difficult to fabricate due to the accumulation of inaccuracies in the alignment of the layers. It is also extremely time consuming to repeat the process multiple times.

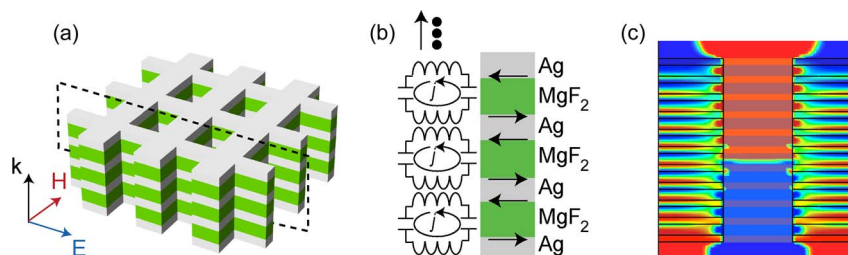


**Fig. 4. Consequences of coupled layers in the bulk fishnet metamaterial. (a) Schematic of a three-functional-layer fishnet showing the cross-section taken in (b) and (c). (b) Depiction of the cascaded circuit that leads to the magnetic response of the structure. Notice that the current flow on the top and bottom surface of the metal is out of phase. (c) Electric field plot of the fishnet generated with FDTD. It can be observed that the electric field on the top and bottom of the metal surfaces is out of phase. This leads to the cancellation of the electric field, and thus current, inside the metal, reducing the losses that occur due to absorption in the metal.**

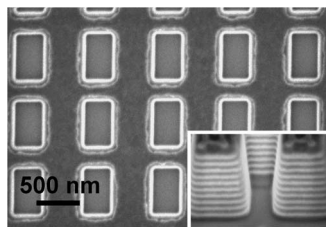


**Fig. 5.** SEM image of the 21-layer fishnet structure with the side etched, showing the cross section. The inset shows a cross section of the pattern taken at a  $45^\circ$  angle. The sidewall angle is  $4.3^\circ$  and was found to have minor effect on the transmittance curve according to simulation. Inset reprinted from [19].

As an alternative to EBL, here we have employed focused ion beam (FIB) milling, which relies on the selective removal of material rather than a deposition/liftoff step. As suggested by the name, the milling of the material is done by a focused ion source, which is usually a liquid metal. The first step is to deposit the device material, which is done with electron beam evaporation. The sample is then placed inside the FIB where a beam is rastered in the areas of the film, which are to be removed. The process flow is considerably less complicated than EBL, and furthermore, is capable of producing features with high aspect ratios, enabling thick metamaterial devices with no alignment steps. The drawbacks of FIB are: 1) it is a relatively slow process compared to EBL and 2) a portion of the milling ions, in this case Gallium, are ultimately embedded into the device material, which introduces extra material loss.

Despite these disadvantages, the high aspect ratios that are capable with FIB make it the ideal tool to achieve a bulk optical NIM. To create the bulk fishnet metamaterial, a multilayer metal-dielectric film stack was first deposited. The multilayer stack was deposited by electron beam evaporation of alternating layers of 30-nm Ag and 50-nm  $\text{MgF}_2$ . The final stack consisted of 21 layers with a total thickness of 830 nm resulting in ten functional layers. The unit cell of the fishnet structure was fabricated with the dimensions outline earlier.

The number of functional layers was chosen in order to establish a convergence of refractive index. The large thickness also allows a prism to be created from the metamaterial as will be discussed later in this section.

Two different configurations of the fishnet samples were fabricated on the multilayer stack. Samples of the first configuration consist of  $22 \times 22$  in-plane fishnet unit cells and were used for the characterization of the transmittance and FOM. A scanning electron microscope (SEM) image of the ten-functional-layer structure is shown in Fig. 5. Samples of the second configuration, which were used to measure the refractive index, consist of a prism fabricated on the multilayer stack, with the number of functional layers ranging from one on one side, to ten on the other side. The prism was formed by placing the sample vertically in the FIB chamber and then tilting the sample at a specified angle  $\beta$  with respect to the film surface, as seen in Fig. 6(a). Once the prism was milled into the surface, the sample was remounted horizontally in the chamber and a  $10 \times 10$  unit cell fishnet pattern was milled into the prism. An atomic force microscope (AFM) and SEM image of the fabricated prism are shown in Fig. 6(b) and (c). The exact angle of the prism was measured with AFM and was found to be slightly varied for different samples.

## V. OPTICAL CHARACTERIZATION AND NUMERICAL SIMULATIONS

To experimentally determine the index of refraction of the metamaterial, measurements were carried out by observing the refraction angle of light passing through the prism, followed by a simple calculation using “Snell’s Law.” This provides a direct and unambiguous determination of the refractive index, as the refraction angle depends solely on the phase gradient the light beam accumulates from propagating through different thicknesses of the material. In the experimental setup, light from an optical parametric oscillator (OPO) was focused onto the prism using an achromatic lens. A second achromatic lens was placed behind the sample with an indium gallium arsenide (InGaAs)

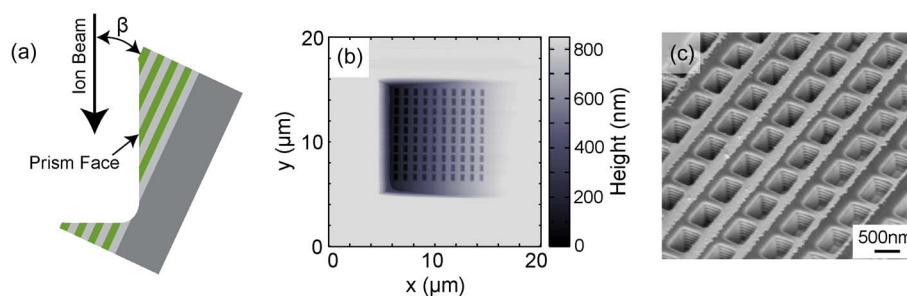


**Fig. 6.** Fabrication procedure and SEM image of the fishnet prism. (a) To fabricate the prism, the multilayer stack was mounted vertically in the FIB and a prism was milled at an angle  $\beta \sim 5^\circ$  with respect to the surface. (b) AFM image of fabricated fishnet prism. (c) SEM image of a fabricated prism with a  $10 \times 10$  unit cell fishnet structure milled into the surface.

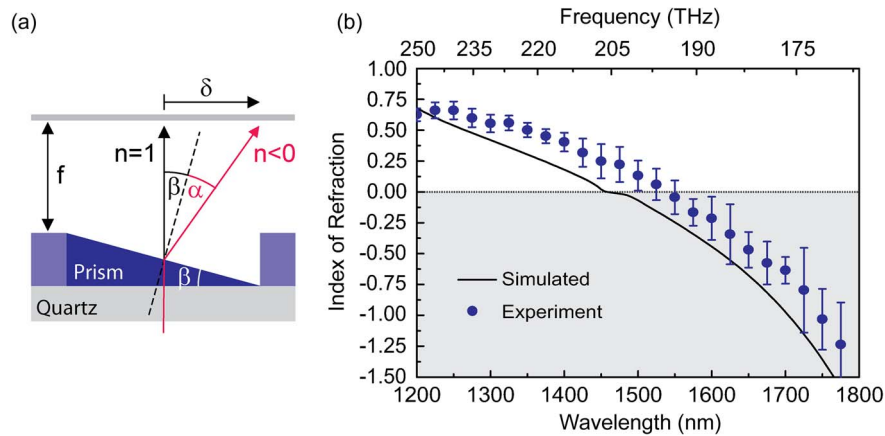
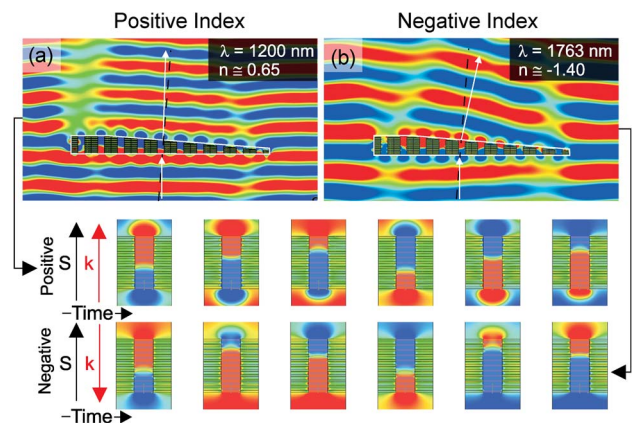


**Fig. 7.** (a) Geometry schematic of the angle measurement.  $\delta$  corresponds to the position difference of the beam passing through a window in the multilayer structure ( $n = 1$ ) and prism sample. By measuring  $\delta$ , the absolute angle of refraction  $\alpha$  can be obtained. (b) Measurements and simulation of the fishnet refractive index. The round dots show the results of the experimental measurement with error bars (standard deviation,  $N = 4$  measurements). The measurement agrees closely with the simulated refractive index using the RCWA method (black line). Reprinted from [19].

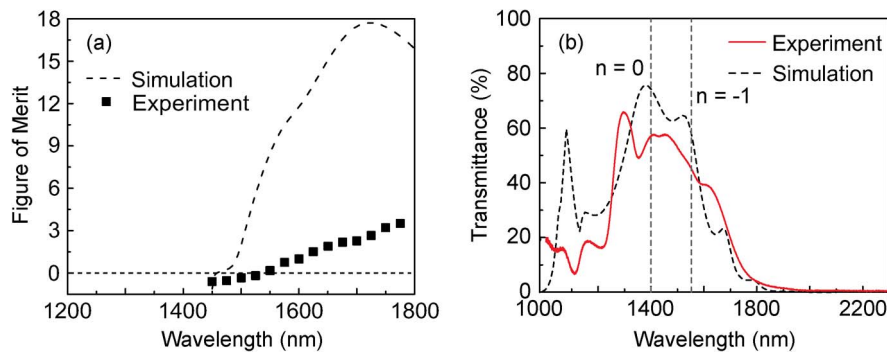
infrared camera placed at the focal position in order to image the Fourier plane [Fig. 7(a)]. The position of the beam at the second lens's focal distance ( $f$ ) was used to calculate the angle of refraction. Due to limited camera imaging area, only the zero-order Fourier image was recorded. To obtain the absolute angle of refraction, a window with an area equal to that of the prism was etched through the multilayer stack to serve as a reference. The window's Fourier image was measured at all wavelengths, giving a reference position corresponding to a refractive index of 1. The centers of the beam spot for both the window and prism samples were determined by fitting the recorded intensity with a 2-D Gaussian profile and the total beam shift ( $\delta$ ) at the position of the second lens was obtained by taking the difference in the two measured beam spot centers. Snell's law,  $n = \sin \alpha / \sin \beta$ , was then used to calculate the real part of the refractive index of the sample.

Fig. 7(b) depicts the measured refractive index of the 3-D fishnet metamaterial at various wavelengths. The refractive index varies from  $n = 0.63 \pm 0.05$  at 1200 nm to  $n = -1.23 \pm 0.34$  at 1775 nm. The refractive index was determined from multiple measurements of two fishnet prisms with angles of  $\beta = 5.0^\circ$  and  $\beta = 4.7^\circ$  and for wavelengths ranging from 1200 to 1800 nm. The experimental results are found to be in good agreement with the theoretical predictions [black line in Fig. 7(b)] based on RCWA. The measured negative refraction angle is a direct result of negative phase evolution for light propagating inside the sample caused by a negative refractive index. This is illustrated in Fig. 8(a) and (b) by a numerical calculation of the in-plane electromagnetic field distribution in the fishnet prism at wavelengths of  $\lambda = 1200$  and 1763 nm where the structure shows a positive and negative index, respectively. Due to the negative phase propagation

inside the metamaterial, the electromagnetic wave emerging from the thicker part of the prism experiences phase advance compared to that passing through the thinner parts, causing the light to bend in the negative direction at the exiting interface. This can be seen in the time-stepped images of the phase within the structure. While phase propagation is in the direction of the Poynting vector when the index is positive, it is opposite at negative indices. We note that the refractive index remains consistent for the



**Fig. 8.** FDTD simulations of light passing through the fishnet prism. (a) Simulation of the in-plane electric field component for the prism structure at 1200 nm when the index is positive. Positive phase propagation results in a positive refraction angle. (b) The in-plane electric field component for the prism structure at 1763 nm showing the phase front of the light. Negative phase propagation resulting from the negative refractive index leads to a negative refraction angle as measured by the beam shift in the experiment. The bottom figures show a closeup of the time evolution of the field distribution in the unit cell for both a positive and negative index of refraction.



**Fig. 9.** FOM of original bulk fishnet and transmission of the fishnet metamaterial on a free-standing membrane. Measurements were performed on  $22 \times 22$  unit cell fishnet structures ( $17.6 \times 17.6 \mu\text{m}^2$  total patterned area). (a) FOM versus wavelength for the simulation (dashed line) and the experiment (black squares). The lower experimental FOM is due to reduced transmission resulting from fabrication imperfections. The experimental FOM reaches 3.5 at 1775 nm where  $\text{Re}(n) = -1.23$ . (b) Experimental (red line) and simulated transmittance (black dotted line) of the bulk fishnet fabricated on a free-standing membrane. Fig. 1(a) reprinted from [19].

fishnet metamaterial with three or more functional layers along the propagation direction, which leads to a uniform wave front exiting the prism. All refractive index measurements of the fishnet are performed at normal incidence as the metamaterial is inherently anisotropic. At large incident angles, the nonlocal effects begin to dominate the response due to the transverse periodicity of the material [30].

In addition, transmittance and reflectance measurements were performed on the bulk fishnet metamaterial in order to calculate the FOM. The sample consisted of ten functional layers and was measured using a Fourier transform infrared microscope (Nicolet Nic-Plan IR microscope). The material loss [i.e.,  $\text{Im}(n)$ ] is conservatively estimated from the measured transmittance and reflectance data by assuming a single pass of light through the metamaterial, as  $\text{Im}(n) = (\lambda/4\pi d) \ln[(1-R)/T]$  where  $\lambda$ ,  $d$ ,  $R$ , and  $T$  are the wavelength, sample thickness, transmittance, and reflectance, respectively. Simulations were performed with RCWA to determine the theoretical FOM. Fig. 9(a) shows the simulated and measured FOM for the bulk fishnet metamaterial. The FOM of the simulated structure reaches a value of 18 at a wavelength of 1750 nm. This FOM is nearly tenfold higher than single-layer NIMs and is due to the combination of magneto-inductive coupling and destructive interference of surface currents in the bulk metamaterial. Experimentally, the transmittance in the negative index band is four times lower than the numerically calculated, yielding an experimental FOM of 3.5 at 1775 nm. The lowered transmission and thus FOM is most likely due to Ga deposition from the FIB. While significantly lower than the theoretical value, this FOM remains among the highest yet achieved at optical frequencies. It should also be noted that transmission measurements were performed with a slightly focused beam resulting in some off normal incident light. Due to the fact that imaginary part of the refractive index increases with

angle of incidence [30], these measurements provide a lower bound for the FOM.

To determine the effect of Ga contamination on the fabricated structure, efforts have been made to minimize the contamination. To accomplish this, bulk fishnet structures has been deposited and milled on top of 50-nm-thick silicon nitride free-standing membranes. By allowing the Ga from the FIB to pass into free space once the pattern is milled, contamination of Ga in the substrate is largely avoided. In this case, the fishnet unit cell dimensions were slightly modified to push the negative index region to shorter wavelengths. The simulated and experimentally measured transmission curves are shown in Fig. 9(b) for a six-functional-layer design with dimensions of  $P_M = P_E = 810$  nm,  $l = 546$  nm,  $w = 278$  nm,  $t = 30$  nm, and  $g = 50$  nm. The measured transmittance exhibits similar features as the calculation, namely, three peaks imposed over the transmission band, which are slightly blue-shifted with respect to the numerical results. These peaks are due to Fabry-Perot effects in which the impedance mismatch leads to reflectance at the metamaterial/air and metamaterial/nitride interfaces. It can be observed that the transmission peak is close to the theoretical value due to the reduced level of Ga contamination in the sample. Work is currently underway to measure the refractive index of the free-standing-membrane-based fishnet structure to determine the experimental FOM.

## VI. OUTLOOK

In his pioneering theoretical work on negative index materials, Veselago proposed a number of exotic phenomena including reversed Doppler effect, backward Cerenkov radiation, and negative radiation pressure [31]. An observation of these effects requires a bulk negative index media, and therefore they have not yet been demonstrated at optical frequencies. With the realization of bulk negative

index materials, exploration of these interesting physics should be within reach. The air apertures in the bulk fishnet metamaterial also allow the access of high energy electrons, and therefore make the observation of reversed Cerenkov radiation possible. Other interesting phenomena that may be demonstrated in a bulk negative index medium include nonlinear processes that involve the nonlinear interaction among optical waves with different signs of the refractive indices owing to the dispersive nature of the metamaterials [32].

Although bulk fishnet metamaterials exhibit much lower loss compared to previous works, they are far from highly transparent. In an effort to decrease the intrinsic loss of metamaterials, several researchers are currently pursuing incorporation of gain material into the underlying structure of the material [33]. Furthermore, the recent reports of plasmonic lasers [34], [35] are an encouraging development that demonstrates the prospects of complete loss compensation in plasmonic metamaterials. ■

## REFERENCES

- [1] D. R. Smith, W. Padilla, D. Vier, S. Nemat-Nasser, and S. Schultz, "Composite medium with simultaneously negative permeability and permittivity," *Phys. Rev. Lett.*, vol. 84, pp. 4184–4187, May 2000.
- [2] R. A. Shelby, D. R. Smith, and S. Schultz, "Experimental verification of a negative index of refraction," *Science*, vol. 292, pp. 77–79, Apr. 2001.
- [3] S. Zhang, W. Fan, N. Panoiu, K. Malloy, R. Osgood, and S. Brueck, "Experimental demonstration of near-infrared negative-index metamaterials," *Phys. Rev. Lett.*, vol. 95, Sep. 2005, 137404.
- [4] V. M. Shalaev, W. Cai, U. K. Chettiar, H.-K. Yuan, A. K. Sarychev, V. P. Drachev, and A. V. Kildishev, "Negative index of refraction in optical metamaterials," *Opt. Lett.*, vol. 30, pp. 3356–3358, Dec. 2005.
- [5] G. Dolling, C. Enkrich, M. Wegener, C. M. Soukoulis, and S. Linden, "Simultaneous negative phase and group velocity of light in a metamaterial," *Science*, vol. 312, pp. 892–894, May 2006.
- [6] J. B. Pendry, "Negative refraction makes a perfect lens," *Phys. Rev. Lett.*, vol. 85, pp. 3966–3969, 2000.
- [7] S. Enoch, G. Tayeb, P. Sabouroux, N. Guérin, and P. Vincent, "A metamaterial for directive emission," *Phys. Rev. Lett.*, vol. 89, Nov. 2002, 213902.
- [8] J. Zhou, T. Koschny, M. Kafesaki, E. Economou, J. Pendry, and C. Soukoulis, "Saturation of the magnetic response of split-ring resonators at optical frequencies," *Phys. Rev. Lett.*, vol. 95, Nov. 2005, 223902.
- [9] A. Ishikawa, T. Tanaka, and S. Kawata, "Negative magnetic permeability in the visible light region," *Phys. Rev. Lett.*, vol. 95, Dec. 2005, 237401.
- [10] S. Zhang, W. Fan, K. J. Malloy, S. R. J. Brueck, N. C. Panoiu, and R. M. Osgood, "Near-infrared double negative metamaterials," *Opt. Exp.*, vol. 13, pp. 4922–4930, Jun. 2005.
- [11] M. Navarro-Cia, M. Beruete, M. Sorolla, and I. Campillo, "Negative refraction in a prism made of stacked subwavelength hole arrays," *Opt. Exp.*, vol. 16, pp. 560–566, Jan. 2008.
- [12] S. Zhang, W. Fan, N. C. Panoiu, K. J. Malloy, R. M. Osgood, and S. R. Brueck, "Optical negative-index bulk metamaterials consisting of 2D perforated metal-dielectric stacks," *Opt. Exp.*, vol. 14, pp. 6778–6787, Jul. 2006.
- [13] J. B. Pendry, L. Martín-Moreno, and F. J. García-Vidal, "Mimicking surface plasmons with structured surfaces," *Science*, vol. 305, pp. 847–848, Aug. 2004.
- [14] A. Mary, S. Rodrigo, F. Garcia-Vidal, and L. Martín-Moreno, "Theory of negative-refractive-index response of double-fishnet structures," *Phys. Rev. Lett.*, vol. 101, Sep. 2008, 103902.
- [15] M. Beruete, M. Navarro-Cía, F. Falcone, I. Campillo, and M. Sorolla, "Single negative birefringence in stacked spoof plasmon metasurfaces by prism experiment," *Opt. Lett.*, vol. 35, pp. 643–645, Feb. 2010.
- [16] G. Dolling, C. Enkrich, M. Wegener, C. M. Soukoulis, and S. Linden, "Low-loss negative-index metamaterial at telecommunication wavelengths," *Opt. Lett.*, vol. 31, pp. 1800–1802, Jun. 2006.
- [17] S. Xiao, U. K. Chettiar, A. V. Kildishev, V. P. Drachev, and V. M. Shalaev, "Yellow-light negative-index metamaterials," *Opt. Lett.*, vol. 34, pp. 3478–3480, Nov. 2009.
- [18] G. Dolling, M. Wegener, C. M. Soukoulis, and S. Linden, "Negative-index metamaterial at 780 nm wavelength," *Opt. Lett.*, vol. 32, pp. 53–55, 2007.
- [19] J. Valentine, S. Zhang, T. Zentgraf, E. Ulin-Avila, D. A. Genov, G. Bartal, and X. Zhang, "Three-dimensional optical metamaterial with a negative refractive index," *Nature*, vol. 455, pp. 376–379, Sep. 2008.
- [20] J. Zhou, T. Koschny, M. Kafesaki, and C. Soukoulis, "Negative refractive index response of weakly and strongly coupled optical metamaterials," *Phys. Rev. B*, vol. 80, Jul. 2009, 035109.
- [21] O. F. Siddiqui and G. V. Eleftheriades, "Periodically loaded transmission line with effective negative refractive index and negative group velocity," *IEEE Trans. Antennas Propag.*, vol. 51, no. 10, pp. 2619–2625, Oct. 2003.
- [22] A. Grbic and G. Eleftheriades, "Overcoming the diffraction limit with a planar left-handed transmission-line lens," *Phys. Rev. Lett.*, vol. 92, Mar. 2004, 117403.
- [23] A. Lai, C. Caroz, and T. Itoh, "Composite right-/left-handed composite transmission line metamaterials," *IEEE Microw. Mag.*, vol. 5, no. 3, pp. 34–50, Sep. 2004.
- [24] G. Dolling, M. Wegener, and S. Linden, "Realization of a three-functional-layer negative-index photonic metamaterial," *Opt. Lett.*, vol. 32, pp. 551–553, Mar. 2007.
- [25] N. Liu, L. Fu, S. Kaiser, H. Schweizer, and H. Giessen, "Plasmonic building blocks for magnetic molecules in three-dimensional optical metamaterials," *Adv. Mater.*, vol. 20, pp. 3859–3865, Oct. 2008.
- [26] N. Liu, H. Guo, L. Fu, S. Kaiser, H. Schweizer, and H. Giessen, "Three-dimensional photonic metamaterials at optical frequencies," *Nature Mater.*, vol. 7, pp. 31–37, Jan. 2008.
- [27] J. Yao, Z. Liu, Y. Liu, Y. Wang, C. Sun, G. Bartal, A. M. Stacy, and X. Zhang, "Optical negative refraction in bulk metamaterials of nanowires," *Science*, vol. 321, p. 930, Aug. 2008.
- [28] A. J. Hoffman, L. Alekseyev, S. S. Howard, K. J. Franz, D. Wasserman, V. A. Podolskiy, E. E. Narimanov, D. L. Sivo, and C. Gmachl, "Negative refraction in semiconductor metamaterials," *Nature Mater.*, vol. 6, pp. 946–950, Dec. 2007.
- [29] J. Yang, C. Sauvan, T. Paul, C. Rockstuhl, F. Lederer, and P. Lalanne, "Retrieving the effective parameters of metamaterials from the single interface scattering problem," *Appl. Phys. Lett.*, vol. 97, 2010, 061102.
- [30] C. Rockstuhl, C. Menzel, T. Paul, T. Pertsch, and F. Lederer, "Light propagation in a fishnet metamaterial," *Phys. Rev. B*, vol. 78, Oct. 2008, 155102.
- [31] V. G. Veselago, "Electrodynamics of substances with simultaneously negative values of sigma and mu," *Soviet Phys. USPEKHI-USSR*, vol. 10, pp. 509–514, 1968.
- [32] A. K. Popov and V. M. Shalaev, "Negative-index metamaterials: Second-harmonic generation, Manley-Rowe relations and parametric amplification," *Appl. Phys. B*, vol. 84, pp. 131–137, Mar. 2006.
- [33] S. Xiao, V. P. Drachev, A. V. Kildishev, X. Ni, U. K. Chettiar, H.-K. Yuan, and V. M. Shalaev, "Loss-free and active optical negative-index metamaterials," *Nature*, vol. 466, pp. 735–738, Aug. 2010.
- [34] R. F. Oulton, V. J. Sorger, T. Zentgraf, R.-M. Ma, C. Gladden, L. Dai, G. Bartal, and X. Zhang, "Plasmon lasers at deep subwavelength scale," *Nature*, vol. 461, pp. 629–632, Oct. 2009.
- [35] M. A. Noginov, G. Zhu, A. M. Belgrave, R. Bakker, V. M. Shalaev, E. E. Narimanov, S. Stout, E. Herz, T. Suteewong, and U. Wiesner, "Demonstration of a spaser-based nanolaser," *Nature*, vol. 460, pp. 1110–1112, Aug. 2009.



### ABOUT THE AUTHORS

**Jason Valentine** received the B.S. degree in mechanical engineering from Purdue University, West Lafayette, IN, in 2004 and the Ph.D. degree in mechanical engineering from the University of California Berkeley, Berkeley, in 2010.

In 2010, he joined the faculty of the Mechanical Engineering Department, Vanderbilt University, Nashville, TN. During his graduate work in Prof. Zhang's laboratory at the University of California Berkeley from 2005 to 2010 he worked on developing optical metamaterials and associated devices. His work includes the development of bulk optical metamaterials as well as the realization of transformation optics inspired devices such as the optical cloak. His current research interests include metamaterials, transformation optics, plasmonics, scalable 3-D manufacturing, photovoltaics, and biological imaging.

Dr. Valentine received the Materials Research Society's Gold Student Award for his work on optical cloaking in 2010. His work has been selected by *Time Magazine* as one of the "Top 10 Scientific Discoveries in 2008."



**Thomas Zentgraf** received the Ph.D. degree from the Faculty of Mathematics and Physics, University of Stuttgart, Stuttgart, Germany, in July 2006.

From 2003 to 2006, he was a Research Assistant at the Max Planck Institute for Solid State Research, Stuttgart, Germany, and in 2005, he was a Visiting Scholar at the Lawrence Berkeley National Laboratory, Berkeley, CA. In 2007, he received a postdoctoral fellowship by the Landesstiftung Baden-Württemberg and shortly afterwards he was awarded with a Feodor Lynen Research Fellowship from the Alexander von Humboldt Foundation to spend two years at the University of California Berkeley, Berkeley, working on metamaterials and transformation optics. Since 2009, he has been a Research Associate in Prof. Zhang's group at the University of California Berkeley. His research interests cover different areas of photonics and optics, such as nonlinear-optical spectroscopy, ultrafast spectroscopy, near-field optical spectroscopy, plasmonic systems, and photonic metamaterials.

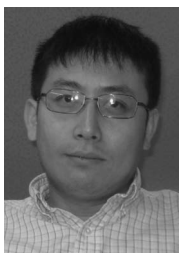
Dr. Zentgraf received the Georg-Simon-Ohm Award of the German Physical Society in 2002 and the Dr.-Heinrich-Düker Award of the Heidehof Foundation in 2006.



**Shuang Zhang** was born in Liaoning Province, China, in 1975. He received the B.S. degree in physics from Jilin University, Changchun, China, in 1993, the M.S. degree in physics from Northeastern University, Boston, MA, in 1999, and the Ph.D. degree in electrical engineering from the University of New Mexico, Albuquerque, in 2005.

From December 2005 to August 2006, he was a Postdoctoral Research Fellow at the University of Illinois at Urbana-Champaign, Urbana, and from August 2006 to March 2010, he was first a Postdoctoral Research Fellow and later an Assistant Research Engineer at the University of California Berkeley, Berkeley. In March 2010, he joined the faculty of the University of Birmingham, Edgbaston, Birmingham, U.K., where he is currently a Reader in the School of Physics and Astronomy.

Dr. Zhang is the recipient of the International Commission for Optics's IUPAP Young Scientist Prize in Optics, 2010 for his research on optical metamaterials. Dr. Zhang's work on macroscopic invisibility cloaking of visible light was selected as one of "top 10 breakthroughs for 2010" by *Physics World*.



**Xiang Zhang** received the Ph.D. degree in mechanical engineering from the University of California Berkeley, Berkeley, in 1996.

He was a faculty member at the Pennsylvania State University and the University of California at Los Angeles prior to joining the Berkeley faculty in 2004. Currently, he is an Ernest S. Kuh Chaired Professor at the University of California Berkeley and the Director of the National Science Foundation (NSF) Nano-Scale Science and Engineering Center (NSEC). He has published more than 180 publications including those in *Science* and *Nature*. He has given over 200 invited, keynote and plenary talks at international conferences and institutions.

Prof. Zhang is an elected member of the U.S. National Academy of Engineering (NAE) and Fellow of the American Physical Society (APS), the Optical Society of America (OSA), the American Association for the Advancement of Science (AAAS), and The International Society for Optical Engineers (SPIE). His group's research in optical metamaterials was selected by *Time Magazine* as "Top 10 Scientific Discoveries in 2008." He is a recipient of an NSF CAREER Award, SME Dell K. Allen Outstanding Young Manufacturing Engineer Award, and an Office of Naval Research (ONR) Young Investigator Award.

